Environmental Science & Technology

Article

pubs.acs.org/est

Phosphate Changes Effect of Humic Acids on TiO_2 Photocatalysis: From Inhibition to Mitigation of Electron−Hole Recombination

Mingce Long,[†,‡] Jonathon Brame,[#] Fan Qin,[§] Jiming Bao,[§] Qilin Li,[*,‡] and Pedro J. J. Alvarez[*,‡]

[†]School of Environmental Science and Engineering, Shanghai Jiao Tong University, Shanghai 200240, China

[‡]Civil and Environmental Engineering, Rice University, Houston, Texas 77005, United States

[§]Department of Electrical & Computer Engineering, University of Houston, Houston, Texas 77204, United States

[#]U.S. Army Engineer Research & Development Center, Vicksburg, Mississippi 39180, United States

Supporting Information

ABSTRACT: A major challenge for photocatalytic water purification with TiO_2 is the strong inhibitory effect of natural organic matter (NOM), which can scavenge photogenerated holes and radicals and occlude ROS generation sites upon adsorption. This study shows that phosphate counteracts the inhibitory effect of humic acids (HA) by decreasing HA adsorption and mitigating electron−hole recombination. As a measure of the inhibitory effect of HA, the ratios of first-order reaction rate constants between photocatalytic phenol degradation in the absence versus presence of HA were calculated. This ratio was very high, up to 5.72 at 30 mg/L HA and pH 4.8 without phosphate, but was decreased to 0.76 (5 mg/L HA, pH 8.4) with 2 mM phosphate. The latter ratio indicates a surprising favorable effect of HA on TiO_2 photocatalysis. FTIR analyses suggest that this favorable effect is likely due to a change in the conformation of adsorbed HA, from a multiligand exchange arrangement to a complexation predominantly between COOH groups in HA and the TiO_2 surface in the presence of phosphate. This configuration can reduce hole consumption and facilitate electron transfer to O_2 by the adsorbed HA (indicated by linear sweep voltammetry), which mitigates electron−hole recombination and enhances contaminant degradation. A decrease in HA surface adsorption and hole scavenging (the predominant inhibitory mechanisms of HA) by phosphate (2 mM) was indicated by a 50% decrease in the photocatalytic degradation rate of HA and 80% decrease in the decay rate coefficient of interfacial-related photooxidation in photocurrent transients. These results, which were validated with other compounds (FFA and cimetidine), indicate that anchoring phosphate - or anions that exert similar effects on the TiO_2 surface - might be a feasible strategy to counteract the inhibitory effect of NOM during photocatalytic water treatment.

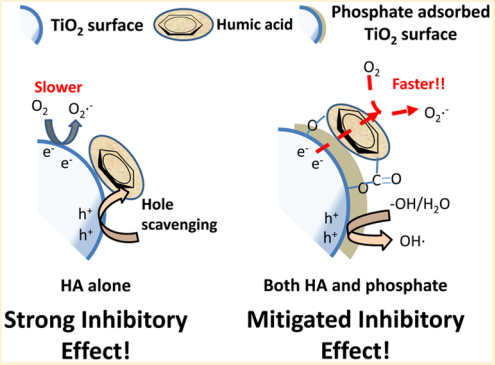

INTRODUCTION

TiO_2 photocatalysis has great potential to be a cost-effective water purification technology for the removal of low concentration recalcitrant organic pollutants, including pharmaceuticals and personal care products (PPCPs).[1−3] However, a notorious obstacle to the efficacy of photocatalytic water treatment is the presence of coexisting constituents, especially dissolved natural organic matter (NOM), which dramatically decrease the degradation efficiency of target pollutants. These inhibitory effects of NOM in photocatalysis and other advanced oxidation processes (AOPs) are widely recognized[4−13] and have been attributed to four mechanisms: (1) decrease in target compound adsorption due to occlusion of active sites on the TiO_2 surface by NOM; (2) decreased generation of reactive oxygen species (ROS) due to NOM adsorption, which interferes with charge transfer; (3) direct competition for ROS (i.e., scavenging); and (4) radiation attenuation, also known as the inner filter effect. The majority of the inhibition is usually attributed to ROS scavenging due to the nonselective nature of hydroxyl radicals (•OH).[11−14]

Several strategies have been developed to address the inhibitory effects of NOM on photocatalysis. These include generating the more electrophilically selective (although less powerful) singlet oxygen as the oxidizing species (e.g., phthalocyanine,[15] porphyrin,[16] or C_{60} aminofullerene photosensitizers[14]), developing the diketone-mediated photochemical oxidation process through a pathway independent of free radicals,[17] and using TiO_2 with a mesoporous structure to restrict access of large NOM molecules.[18] However, these methods generally yield lower contaminant removal efficiency or higher photocatalyst cost. Therefore, achieving high removal efficiency of priority organic pollutants during TiO_2-based

Received: September 23, 2016
Revised: December 1, 2016
Accepted: December 6, 2016
Published: December 6, 2016

DOI: 10.1021/acs.est.6b04845
Environ. Sci. Technol. 2017, 51, 514−521

photocatalytic treatment of natural water or wastewater remains a critical challenge.

Unlike homogeneous photoreactions, catalyst surface properties play an important role in heterogeneous photocatalysis. In a well-mixed, evenly irradiated homogeneous system, such as H_2O_2 irradiated by UVC, •OH is generated uniformly throughout the solution. Therefore, competition between NOM and target chemicals primarily depends on the respective reaction rate coefficients with •OH.[19] In contrast, in a heterogeneous system such as those involving TiO_2, ROS are generated at the irradiated surface of the photocatalyst, and the produced ROS have very short diffusion lengths (e.g., tens of nm with mM substrate concentrations).[20,21] Most reactions between ROS and organics must therefore take place within close proximity to the TiO_2 surface, and adsorption of substrates onto TiO_2 surface is frequently a crucial factor in photocatalytic degradation.

While most priority hydrophilic micropollutants display low tendency to adsorb onto TiO_2,[22,23] humic acid (HA), a representative NOM and among the most frequently existing organic compounds in water, possesses abundant phenolic, hydroxyl, or carboxylic groups that facilitate its adsorption onto TiO_2.[24] Thus, the photocatalytic degradation of target priority chemicals can be greatly suppressed by HA in the TiO_2 suspension. Photocatalytic degradation of organic compounds can also be influenced by the presence of some anions, such as phosphate or fluoride, which bind onto the TiO_2 surface and alter the surface adsorption capacity for the target organic compounds. It has been shown that this influence depends strongly on the adsorption capacity of the target organic compound onto TiO_2.[22,25] For example, phosphate increases the degradation rates for compounds that adsorb poorly on TiO_2 by enhancing ROS generation; however, phosphate inhibits the degradation of compounds with strong adsorption by hindering direct hole oxidation.[22] The combined effects of both anions and HA on the degradation of target organic pollutants has not been fully characterized and may provide a method whereby inhibitory effects of HA adsorption can be abated by anion sorption.

In this paper, we investigate the counteracting influence of phosphate on the inhibitory effect of humic acid (HA) during photocatalytic degradation of organic pollutants (e.g., phenol). We propose a strategy to explain these effects, based on the effects of phosphate on the TiO_2 surface. Using photocurrent measurements, FTIR spectra and kinetic analyses, we show that phosphate counteracts the inhibitory effect of HA by (1) decreasing adsorption of HA, which reduces hole scavenging, and (2) changing the adsorbed HA conformation in a manner that facilitates electron transfer and suppresses photogenerated charge recombination.

EXPERIMENTAL METHODS

Materials. Humic acid in the sodium salt form, furfuryl alcohol (FFA), phenol, cimetidine, NaH_2PO_4, Na_2HPO_4, $NaClO_4$, and other chemicals were all obtained from Sigma-Aldrich and used without further purification. TiO_2 (Degussa P25) was used in all tests. Initial pH of each solution or suspension was carefully adjusted using $HClO_4$ or NaOH or maintained using a phosphate buffer.

Photocatalytic Degradation Experiments. All reactions took place in a magnetically stirred quartz reactor described previously.[12−14] Six 4 W UVA bulbs (Sankyo Denki FL4BLB, 350−400 nm, 18 mW cm^{-2}) aligned in two rows (three bulbs per row) were used as light sources. The light intensity inside the reactor was 452 $\mu W/cm^2$ (365 nm), measured with a UV-A radiometer (Beijing Normal University Optronics Factory, Beijing, China). HA was used as a model for NOM in all experiments. To determine the inhibitory effect of HA toward photocatalytic degradation of target pollutants, 50 mL TiO_2 suspensions (0.5 g/L) were mixed in a quartz reaction vessel with organic pollutants (10 mg/L phenol), and then varied amounts of HA were added immediately.

To evaluate the role of phosphate, a NaH_2PO_4 solution (0.1 M) was used to prepare the TiO_2 suspension. The pH of the suspension was adjusted to a desired value. The mixture of TiO_2, organic pollutant, HA, and phosphate was stirred in the dark for 20 min to allow adsorption equilibrium, and an initial sample was taken. Adsorption kinetics tests showed that 20 min was sufficient for adsorption equilibrium (Figure S1). Then the suspension was illuminated, and samples were withdrawn at predetermined times, filtered through a 0.45-μm PES filter (Millipore), and analyzed for the target compound concentration by HPLC. The photocatalytic degradation of HA was tested using the same experimental procedure at an initial solution pH of 6.20 and an initial HA concentration of 20 mg/L. HA concentration was determined by measuring absorbance at 254 nm and calibrating with standard samples with known HA concentrations using an Ultraspec 2100 Pro UV/vis spectrophotometer (Amersham Biosciences, USA) with a 1 cm quartz cuvette (Figure S2). Note that absorbance at 254 nm may disproportionally represent some chromophoric fractions of HA associated with aromatic or double-bonded structures.[26] Nevertheless, this chromophoric fraction has been shown to have a significant effect on TiO_2 photocatalysis.[26−28]

Kinetic Analyses. Apparent first-order degradation rate constants (k) were obtained for all photocatalytic processes by nonlinear regression of concentration versus time data. In the presence of phosphate, the first-order phenol degradation rate constant obtained at the same phosphate concentration but in the absence of HA was used as k_0. The ratio (R) between the reaction rate constants in the absence (k_0) and presence of HA (k) was used as a measure of the inhibitory effect of HA. An R value of 1 suggests no influence of HA on the photocatalytic degradation rate of the target compound ($k_0 = k$), while a value >1 ($k_0 > k$) indicates inhibitory effects.

When the •OH concentration is far less than the concentration of the substrates (which is generally the case here), the theoretical R value (R_T) is mainly determined by the reaction rate constants for phenol and HA and their concentrations (eq 1)

$$R_T = 1 + k_{HA}C_{HA}/k_{Phenol}C_{Phenol} \quad (1)$$

where k_{HA} and k_{Phenol} are the respective rate constants for HA and phenol reacting with •OH, and C_{HA} and C_{Phenol} are the initial concentrations of HA and phenol.[29] Note that R_T calculated by eq 1 represents inhibition due to ROS scavenging only.

Analytical Methods. Quantitative analyses of the residual concentrations of target substrates were performed using a HPLC (Shimadzu LC-20AD) equipped with a C-18 column (ZORBAX Eclipse XDB-C18) and an UV−vis detector (SPD-20AV). The mobile phase is comprised of a binary mixture of 0.1 wt % aqueous phosphoric acid solution and acetonitrile at the ratio of 70:30, 45:55, and 90:10 by volume for FFA, phenol, and cimetidine, respectively. The flow rates were 1.0 and 0.6 mL/min for FFA and phenol, respectively, and the detection

DOI: 10.1021/acs.est.6b04845
Environ. Sci. Technol. 2017, 51, 514−521

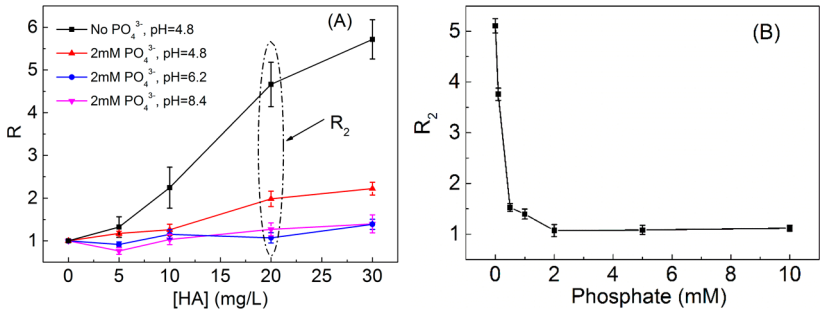

Figure 1. Effect of phosphate on the photocatalytic degradation kinetics of phenol. Panel (A) shows the ratio of reaction rate constants R, which is the ratio between the reaction rate constants in the absence and presence of HA, with varying HA concentrations. Panel (B) shows the effect of phosphate concentration on R_2 (i.e., the R value when the HA concentration is twice that of phenol) at pH 6.2. Error bars represent standard deviations from the mean of triplicates.

wavelength was 230 nm for all compounds. The infrared spectra of HA adsorbed on TiO_2 was recorded on a Fourier transform infrared (FTIR) spectrometer (Nicolet 6700). HA bound TiO_2 (HA/TiO_2) samples were prepared using a suspension containing 20 mg/L HA and 0.5 g/L TiO_2 at pH 6.2, while the HA bound TiO_2 in the presence of phosphate (HA/phosphate/TiO_2) was prepared in a suspension of 40 mg/L HA in 0.5 g/L TiO_2 with 2 mM phosphate. The solid was separated by filtration and freeze-dried for measurement.

Photoelectrochemical Tests. The reaction pathway of direct oxidation by holes was investigated by photocurrent measurement using a 263A Princeton Applied Research (PAR) potentiostat/galvanostat in combination with a PAR M5210 lock-in amplifier. The working electrodes were prepared on indium tin oxide (ITO) glass plates (Adafruit, USA, 1.1 mm thick, sheet resistance of 10−15 Ω per sq inch). Degussa P25 powder (200 mg) was suspended in 1 mL of absolute ethanol and cast over an area of 2.5 cm × 2.5 cm on the cleaned ITO glass substrate. The electrodes were then heated at 400 °C in air for 2 h. A three-electrode setup (Figure S3) was used in all measurements with a platinum wire as the counter electrode and Ag/AgCl (in 3.0 M NaCl solution) as the reference electrode connected to the electrolyte solution by a salt bridge. The light source for photocurrent measurements was a Thorlabs high power 365 nm UV LED operating nominally at 250 mW/cm^2 power output. The electrolyte was a 15 mL 0.1 M $NaClO_4$ solution at pH 5.9. The solution was purged with nitrogen for 10 min prior to each measurement and continuously purged during the measurement.

Electrochemical Tests. To evaluate the oxygen reduction reaction on TiO_2, linear sweep voltammetry was performed in the dark in 15 mL nitrogen-purged or O_2-saturated 0.1 M $NaClO_4$ solution (pH was adjusted to 3.5 with 1 M $HClO_4$) with or without 20 mg/L HA. The working electrode and three-electrode setup were the same as those in photoelectrochemical tests but without light irradiation. Phosphate modified TiO_2 film was prepared by immersing the TiO_2 film in 0.1 M NaH_2PO_4 solutions (pH = 3.5) overnight and following the same calcination procedure as for the TiO_2 film.[30]

Statistical Analysis. Triplicate experiments were carried out for each test, and error was measured as standard deviations from the mean. Student's paired t test (single-tailed) was used to assess the significance of the differences between treatments at the 95% confidence level ($p < 0.05$). The standard error of R was calculated using propagation of error analyses according to eq S2.

RESULTS AND DISCUSSION

Phosphate Counteracts the Inhibitory Effect of HA. Figure 1 shows the effect of HA on phenol degradation kinetics in the presence and absence of phosphate. Without phosphate, HA had a strong inhibitory effect on phenol degradation ($R > 1$, Figure 1A) at unadjusted pH (pH 4.8). The inhibitory effect increased with HA concentration, with R values as high as 5.72 (±0.54, $p < 0.05$) with 30 mg/L HA. Whereas NOM and other factors (e.g., pH, ionic strength) could affect TiO_2 aggregation, previous studies have shown that aggregation does not significantly change the adsorption characteristics of organic acids onto TiO_2.[31] Thus, potential changes in TiO_2 aggregation are not expected to significantly affect photocatalytic degradation rates in these experiments.

Interestingly, phosphate significantly reduced the inhibitory effect of HA as suggested by the notably lower R values (Figure 1A, $R < 2$ in the presence of phosphate). In fact, phosphate alone increased the phenol degradation rate: the apparent first-order reaction rate coefficient nearly doubled from 0.029 (±0.0004) to 0.056 (±0.0006) min^{-1} with 0.1 mM phosphate added or 0.069 (±0.001) min^{-1} ($p < 0.05$) with 2 mM phosphate added (Figure S4). However, the R values here are normalized to the degradation rate constant in the presence of phosphate (0.069 min^{-1}, with no HA). The counteracting effect of phosphate was greater at higher pH (Figure 1A). At pH 6.2 and 8.4, HA concentrations up to 30 mg/L had minimal impact on phenol degradation rate when 2 mM phosphate was present, with R values as low as 1.39 and 1.40, respectively. This can be attributed to the combined effects of phosphate and higher pH, both of which contribute to decreasing adsorption of HA onto the TiO_2 surface.[24] In the absence of phosphate and HA, phenol degradation rates in the pH range tested do not change significantly (Figure S5). Moreover, the inhibitory effect of HA decreased with increasing phosphate concentration. As shown in Figure 1B, R_2 (the R value when the HA concentration is twice that of phenol) at pH 6.2 decreased significantly from 5.10 to 1.52 when 0.5 mM phosphate was added and approached unity as phosphate concentration increased to 2 mM. The counteracting effect of phosphate was also observed in the photocatalytic degradation of two other compounds, FFA and cimetidine (Figure S6). In the presence of 2 mM phosphate, R values decreased to 1.12 (±0.08, $p < 0.05$) for FFA and 1.08 (±0.05, $p < 0.05$) for cimetidine. Such a counteracting effect of phosphate was not observed in the homogeneous H_2O_2/UVC advanced oxidation system (Figure S7), suggesting minimal interaction of phosphate with •OH in the bulk solution.

DOI: 10.1021/acs.est.6b04845
Environ. Sci. Technol. 2017, 51, 514−521

Competitive Sorption between Phosphate and HA. Phosphate anions can adsorb strongly onto TiO_2, with a Langmuir binding constant as high as 0.4 ± 0.08 L mg^{-1} (at pH 2.3), which is comparable to that of bidentate ligands such as oxalate and catechol.[32] This binding constant is also comparable to that of HA (0.12 to 0.90 L mg^{-1} at pH 6.5).[33,34] Hence, phosphate can compete with HA for adsorption sites on the TiO_2 surface. When both phosphate and HA are present in the system, phosphate can competitively displace some of the adsorbed HA, thereby decreasing hole scavenging by adsorbed HA. As shown in Figure 2, the degradation rate constant of HA an initial concentration of 20 mg/L was 0.024 (±0.0004) min^{-1} (as measured by decreased absorbance at 254 nm). When 2 mM phosphate was added, the degradation rate constant decreased by 50% to 0.012 (±0.0003) min^{-1} ($p < 0.05$). Additionally, in the presence of 2 mM phosphate, the adsorption capacity of HA onto the TiO_2 surface was reduced by 75% (Figure S8), suggesting that HA degradation by direct hole oxidation should decrease but could remain a contributing factor. Although the presence of 2 mM phosphate both inhibited degradation of HA and accelerated degradation of phenol, their degradation rate constants (0.012 (±0.0003) min^{-1} ($p < 0.05$) for HA and 0.069 (±0.001) min^{-1} ($p < 0.05$) for phenol) were still comparable, indicating that ROS scavenging by HA during phenol degradation could be notable even in the presence of phosphate.

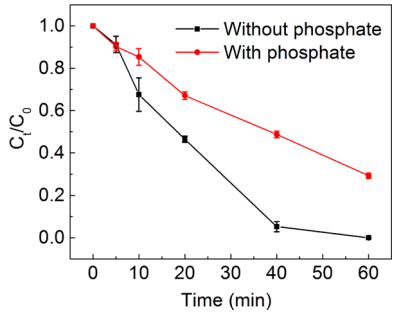

Figure 2. Photocatalytic degradation of HA ($[HA]_0$ = 20 mg/L) with TiO_2 in the presence and absence of 2 mM phosphate at initial pH 6.2.

The effect of competitive sorption was further investigated by measuring photocurrent (Figure 3). The initial photocurrent spike is an indication of surface recombination of photo-generated electrons and holes due to the slower transfer rate of holes for water oxidation, while the steady state photocurrent corresponds to photoelectrochemical activity of semiconductor electrodes.[35−37] In the blank $NaClO_4$ solution (curve a), a steady state photocurrent density of ∼500 $\mu A/cm^2$ was measured. The lower steady state photocurrent in the presence of phosphate (curve b) is attributed to the retarded water oxidation by adsorbed phosphate ions on the TiO_2 surface.[35] With the addition of HA (curve c), photocurrent profiles displayed a notably larger peak, indicating the capture of surface photogenerated holes by HA and a corresponding increase in electron transfer.[38−40] In the presence of organics, the photocurrent profile (I_{ph}) could be described using a double-exponential model (eq 2)[39]

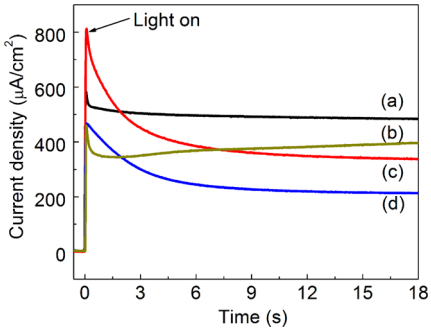

Figure 3. Time dependent photocurrent generation by TiO_2 films in 0.1 M $NaClO_4$ at 0.2 V versus Ag/AgCl with various combinations of phosphate (2 mM) and HA (20 mg/L): (a) control (no phosphate or HA); (b) phosphate alone; (c) HA alone; and (d) phosphate and HA. Solutions were purged with N_2.

$$I_{ph} = I_0 + A \exp(-k_1 t) + B \exp(-k_2 t) \quad (2)$$

where the two exponential decay terms correspond to the slow interfacial-related and the fast surface-related photocatalytic reactions, respectively. A and B indicate the instantaneous initial rates of these two reactions, whose respective rate constants are k_1 and k_2 (Text S5).

The double-exponential model (eq 2) fits the data (curves c and d in Figure 4) quite well (Figure S9). With HA alone (curve c), the parameters k_1 and k_2 were 0.242 (±0.002) and 0.971 (±0.011) s^{-1}, respectively; with both HA and phosphate (curve d), they were 0.047 (±0.001) and 0.406 (±0.001) s^{-1}, respectively. The decay rate constants in the presence of phosphate decreased by 80% for the slow (interfacial-related) and by 58% for the fast (surface related) processes. This suggests that HA oxidation by photogenerated holes is greatly suppressed by phosphate. The charges calculated from integrating the spike photocurrent of curves c and d (Figure S10) represent charge transfer to HA adsorbed on the electrode,[40] which are 6675 and 4562 μC, respectively. The decrease in charge transfer is a result of a decrease in both adsorption and hole oxidation of HA in the presence of 2 mM phosphate. Photocurrent transients show some remaining adsorption and oxidation of HA taking place, which indicates that the presence of phosphate did not completely preclude the adsorption and inhibitory effect of HA on TiO_2 photocatalysis.

Facilitated Electron Transfer by Adsorbed HA. Due to the relatively low light absorption of HA in the UVA range (350−400 nm) and the negligible phenol adsorption on TiO_2, radiation attenuation and competitive surface adsorption are not expected to be important contributors to the inhibitory effect of HA on phenol degradation.[13] The inhibitory effect of HA is therefore mainly attributed to the competitive reaction with ROS and the decreased ROS production due to hole scavenging by surface adsorbed HA molecules.[12,13] The former can be estimated from the competitive reactions of HA and phenol with ROS, especially hydroxyl radicals. HA in suspension competes with phenol for available •OH, irrespective of phosphate. To make the ratio comparable, all units were converted into (mg of C L^{-1}). The rate constant for k_{Phenol} is 1.8×10^{10} M^{-1} s^{-1} at pH 6−7, corresponding to 2.5×10^5 (mg of C $L^{-1})^{-1}$ s^{-1}. The reported rate constant for k_{HA} is in the range of $(1.5–3.0) \times 10^4$ (mg of C $L^{-1})^{-1}$ s^{-1},[7,8,41] which is ten times smaller than k_{Phenol}. Considering the carbon content in HA (about 50%), the R_{T2} calculated from eq 1 was only 1.13, which is much lower than the measured R_2 value of 5.1 at pH 6.2 (Figure 1B). Since the measured R_2 value is so much higher than the R_{T2} value calculated from ROS production rate constants (eq 2), the scavenging of produced ROS does not

DOI: 10.1021/acs.est.6b04845
Environ. Sci. Technol. 2017, 51, 514−521

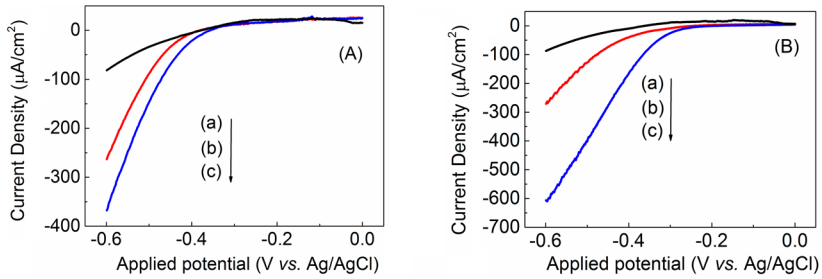

Figure 4. Linear sweep voltammetry (50 mV s^{-1}) of TiO_2 film (A) and phosphate modified TiO_2 film (B) in 0.1 M $NaClO_4$ solution (pH = 3.5) under various conditions: (a) control (nitrogen-purged); (b) oxygen-saturated; (c) oxygen-saturated in the presence of 20 mg/L HA.

account for the majority of the inhibitory effect, which is consistent with previous work.[7,8] This suggests that decreased ROS production due to hole scavenging by adsorbed HA was the predominant mechanism for the inhibitory effect of HA on phenol degradation.

Considering the competitive reaction with ROS and the remaining sorption of HA, the inhibitory effect of HA would still be significant, even with the addition of phosphate. Interestingly, the R values were very low at pH 6.2 and 8.4, and R_2 is only 1.07 (±0.12) ($p < 0.05$) at pH 6.2. Most notably at 5 mg/L HA, R is even less than 1 in the presence of 2 mM phosphate, with values of 0.913 (±0.06) ($p < 0.05$) at pH 6.2 and 0.763 (±0.08) ($p < 0.05$) at pH 8.4 (Figure 1A). This reflects the enhanced phenol degradation shown in Figure S11. The presence of HA (6 mg/L) has also been reported to increase the photocatalytic degradation of quinolone on TiO_2.[9] All these results suggest that there exists a mechanism through which HA enhances (albeit slightly) phenol degradation in the presence of phosphate, and this mechanism compensates for HA's inhibitory effect in photocatalysis.

There are two possible mechanisms for the observed enhanced degradation of organic pollutants in the presence of HA. The first is that energy can be transferred from excited HA to oxygen to produce singlet oxygen ($^1O_2$). However, experiments using FFA as a probe for $^1O_2$ production under both UVA and UVC irradiation showed negligible enhancement of FFA removal in the presence of HA (Figure S12). The low quantum yield of $^1O_2$ from HA excitation in this system apparently contributes negligibly to phenol degradation. The other possible mechanism is that under certain circumstances, HA can enhance electron transfer to oxygen to prevent electron−hole recombination and enhance photocatalytic degradation. Generally, the photocatalytic reaction rate is significantly influenced by the recombination of photogenerated carriers, and the electron transfer and capture by oxygen is regarded as the rate-determining step in the reaction.[42,43] Therefore, enhanced electron transfer to O_2 is an important mechanism to suppress electron−hole recombination and accordingly improve the efficiency for organic degradation.

The roles of phosphate and HA in electron transfer were studied by linear sweep voltammetry, measuring the oxygen reduction reaction (ORR) rate on the surface of a TiO_2 film electrode (Figure 4). The cathodic current density measured represents the ORR rate on the working electrode. As shown in Figure 4A, the electrochemical ORR in an oxygen saturated solution was slightly enhanced by HA addition, with the cathodic current density increasing from −264 $\mu A/cm^2$ to −367 $\mu A/cm^2$ at a bias of −0.6 V vs Ag/AgCl. This suggests that HA facilitates electron transfer from the TiO_2 surface to oxygen. However, HA alone did not enhance phenol degradation. Apparently, the negative effect of hole scavenging by adsorbed HA outweighs the enhanced electron transfer. In the presence of HA, however, phosphate-modified TiO_2 displayed a much greater increase in ORR, with the cathodic current density increasing from −274 $\mu A/cm^2$ to −608 $\mu A/cm^2$ at a bias of −0.6 V vs Ag/AgCl. This favorable effect more than compensated for the negative impact of HA through hole scavenging, leading to increased phenol degradation.

FTIR analyses of HA adsorbed on TiO_2 surface (Figure 5) suggest that the large enhancement in electron transfer may be

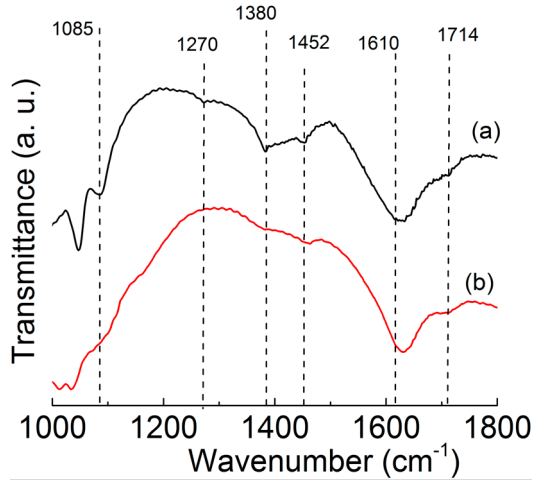

Figure 5. FTIR spectra (1000−1800 cm^{-1}) of HA adsorption on TiO_2 in the absence (a) and presence (b) of phosphate (2 mM, pH = 6.2).

attributed to changes in the adsorbed states of bound HA molecules. In the presence of 40 mg/L HA and 2 mM phosphate, the adsorption of HA was 12.4 (±2.5) ($p < 0.05$) mg/g, comparable to the adsorption in the presence of 20 mg/L HA alone (15.9 (±2.3) ($p < 0.05$) mg/g (Figure S8). However, the FTIR spectra of adsorbed HA in the presence and absence of phosphate exhibit several differences. In the absence of phosphate, the shoulder around 1085 cm^{-1} is attributed to the adsorbed aliphatic fractions, such as polysaccharide-like substances,[44,45] the peak at 1270 cm^{-1} is attributed to the C−OH stretch of phenolic OH, and those at 1380, 1452, 1610, and 1714 cm^{-1} are assigned to in-plane bending vibration of OH, coupled C−O stretching, COO asymmetric stretching, and C═O stretching, respectively, from carboxylate groups in HA.[44,45] This is consistent with previous findings that both aromatic and aliphatic fractions of HA adsorb on TiO_2 through ligand exchanges with phenolate and carboxylate groups or by hydrophobic interactions.[24,44] In the

DOI: 10.1021/acs.est.6b04845
Environ. Sci. Technol. 2017, 51, 514−521

presence of phosphate, the peaks at 1270 and 1610 cm^{-1} diminished, the peak intensity at 1380 and 1714 cm^{-1} decreased, and the peak at 1452 cm^{-1} shifted to 1460 cm^{-1}. These results collectively indicate strong bonding between TiO_2 surface and hydroxyl and carboxyl groups of HA in the presence of phosphate.

We postulate that the presence of phosphate changes the binding of HA molecules to the TiO_2 surface and hence affects the electron shuttling property of HA. Both AFM studies[46] and theoretical calculations[9] have suggested that (in the absence of phosphate) HA molecules adsorb primarily with the electron-donating aromatic rings parallel to the TiO_2 surface (as shown in the TOC art). In this adsorbed state, HA molecules are efficient hole scavengers with the aromatic rings serving as electron donors.[47,48] Phosphate adsorption on TiO_2 leads to a more hydrophilic and negatively charged surface (pH of the zero point of charge, $pH_{zpc} \sim 2.3$).[25] We propose that HA adsorption in the presence of phosphate mainly occurs through Ti(IV) complexation with the −COOH and −OH groups on HA, which promotes interfacial electron transfer[30,49] and reduces hole scavenging as the aromatic rings are further away from the surface (see the TOC Art). These effects could partially or even completely compensate for HA's inhibitory effect on photocatalysis.

In summary, the mechanisms by which phosphate counteracts the inhibitory effect of HA on TiO_2 photocatalysis involve (1) decreased adsorption of HA, which reduces hole scavenging, and (2) changes in the adsorption state of HA molecules to TiO_2 surface, which facilitates electron transfer and suppresses photogenerated charge recombination.

Technological Implications. We proposed a potential strategy to counteract the detrimental effect of NOM on TiO_2 photocatalysis, based on exploiting the effects of phosphate on the TiO_2 surface. Specifically, kinetic analyses show that HA can exert both inhibitory and favorable effects on TiO_2 photocatalysis. The inhibitory effect is mainly attributed to hole scavenging by HA molecules adsorbed onto the TiO_2 surface, and is often predominant. The favorable effect is due to enhanced electron transfer to O_2 facilitated by HA molecules adsorbed through complexation between Ti(IV) and carboxyl and hydroxyl groups in HA, which suppresses charge recombination. The presence of phosphate not only reduces HA adsorption and hence direct hole scavenging by HA but also enhances HA-facilitated electron transfer by changing the adsorbed state of HA, resulting in significantly increased photocatalytic degradation rates for various organic compounds. Accordingly, phosphate could be anchored on the TiO_2 surface to offset the inhibitory effect of NOM (and potentially enable its positive effect in mitigating charge recombination) to carry out efficient photocatalytic degradation of priority organic pollutants. Other anions such as sulfate are also pervasive in water, which underscores the importance to advance mechanistic understanding of their effects on TiO_2 surface chemistry to discern how photocatalytic performance is affected by water chemistry and to guide TiO_2 surface modification strategies that counteract common inhibitory effects by NOM.

■ ASSOCIATED CONTENT

Supporting Information

This material is available free of charge via the Internet at http://pubs.acs.org/. The Supporting Information is available free of charge on the ACS Publications website at DOI: 10.1021/acs.est.6b04845.

Time dependent adsorption of HA on TiO_2 (Figure S1), standard curve for the relationship between HA and SUV_{254} absorbance (Figure S2), three-electrode setup for photoelectrochemical or electrochemical tests (Figure S3), effect of phosphate concentration on phenol degradation (Figure S4), comparison of phenol degradation (Figure S5), phosphate addition during photocatalytic degradation of FFA or cimetidine (Figure S6), first-order phenol degradation rate constant with H_2O_2 (Figure S7), adsorption of HA over TiO_2 (Figure S8), fitting results and parameters for the photocurrent decay of (Figure S9) and integrated spike photocurrent of (Figure S10) curves c and d in Figure 2 , photocatalytic degradation of phenol with TiO_2 (Figure S11), photolytic degradation of FFA using UVA and UVC light (Figure S12), FTIR spectra of HA adsorption on TiO_2 (Figure S13) (PDF)

■ AUTHOR INFORMATION

Corresponding Authors

*Phone: 713-348-2046. Fax: 713-348-5268. E-mail: Qilin.Li@rice.edu (Q.L.).

*Phone: 713-348-5903. Fax: 713-348-5203. E-mail: alvarez@rice.edu (P.J.J.A.).

ORCID

Jiming Bao: 0000-0002-6819-0117

Pedro J. J. Alvarez: 0000-0002-6725-7199

Notes

The authors declare no competing financial interest.

■ ACKNOWLEDGMENTS

This work is financially supported by the National Natural Science Foundation of China (No. 21377084), Shanghai Municipal International Cooperation Foundation (No. 15230724600), and the NSF ERC on Nanotechnology-Enabled Water Treatment (EEC-1449500).

■ REFERENCES

(1) Carbonaro, S.; Sugihara, M. N.; Strathmann, T. J. Continuous-flow photocatalytic treatment of pharmaceutical micropollutants: Activity, inhibition, and deactivation of TiO_2 photocatalysts in wastewater effluent. *Appl. Catal., B* **2013**, *129*, 1−12.

(2) Fang, H.; Gao, Y.; Li, G.; An, J.; Wong, P. K.; Fu, H.; Yao, S.; Nie, X.; An, T. Advanced oxidation kinetics and mechanism of preservative propylparaben degradation in aqueous suspension of TiO_2 and risk assessment of its degradation products. *Environ. Sci. Technol.* **2013**, *47* (6), 2704−2712.

(3) Michael, I.; Hapeshi, E.; Osorio, V.; Perez, S.; Petrovic, M.; Zapata, A.; Malato, S.; Barcelo, D.; Fatta-Kassinos, D. Solar photocatalytic treatment of trimethoprim in four environmental matrices at a pilot scale: Transformation products and ecotoxicity evaluation. *Sci. Total Environ.* **2012**, *430*, 167−173.

(4) Selli, E.; Baglio, D.; Montanarella, L.; Bidoglio, G. Role of humic acids in the TiO_2-photocatalyzed degradation of tetrachloroethene in water. *Water Res.* **1999**, *33* (8), 1827−1836.

(5) Minero, C.; Pelizzetti, E.; Sega, M.; Friberg, S. E.; Sjöblom, J. The role of humic substances in the photocatalytic degradation of water contaminants. *J. Dispersion Sci. Technol.* **1999**, *20* (1−2), 643−661.

(6) Westerhoff, P.; Aiken, G.; Amy, G.; Debroux, J. Relationships between the structure of natural organic matter and its reactivity

DOI: 10.1021/acs.est.6b04845
Environ. Sci. Technol. 2017, 51, 514−521

towards molecular ozone and hydroxyl radicals. *Water Res.* **1999**, *33* (10), 2265−2276.
(7) Lindsey, M. E.; Tarr, M. A. Inhibited hydroxyl radical degradation of aromatic hydrocarbons in the presence of dissolved fulvic acid. *Water Res.* **2000**, *34* (8), 2385−2389.
(8) Lindsey, M. E.; Tarr, M. A. Inhibition of hydroxyl radical reaction with aromatics by dissolved natural organic matter. *Environ. Sci. Technol.* **2000**, *34* (3), 444−449.
(9) Enriquez, R.; Pichat, P. Interactions of humic acid, quinoline, and TiO_2 in water in relation to quinoline photocatalytic removal. *Langmuir* **2001**, *17* (20), 6132−6137.
(10) Doll, T. E.; Frimmel, F. H. Photocatalytic degradation of carbamazepine, clofibric acid and iomeprol with P25 and Hombikat UV100 in the presence of natural organic matter (NOM) and other organic water constituents. *Water Res.* **2005**, *39* (2−3), 403−11.
(11) Lee, Y.; von Gunten, U. Oxidative transformation of micropollutants during municipal wastewater treatment: Comparison of kinetic aspects of selective (chlorine, chlorine dioxide, ferrateVI, and ozone) and non-selective oxidants (hydroxyl radical). *Water Res.* **2010**, *44* (2), 555−566.
(12) Brame, J.; Long, M.; Li, Q.; Alvarez, P. Trading oxidation power for efficiency: differential inhibition of photo-generated hydroxyl radicals versus singlet oxygen. *Water Res.* **2014**, *60*, 259−266.
(13) Brame, J.; Long, M.; Li, Q.; Alvarez, P. Inhibitory effect of natural organic matter or other background constituents on photocatalytic advanced oxidation processes: Mechanistic model development and validation. *Water Res.* **2015**, *84*, 362−371.
(14) Kim, H.; Kim, W.; Mackeyev, Y.; Lee, G. S.; Kim, H. J.; Tachikawa, T.; Hong, S.; Lee, S.; Kim, J.; Wilson, L. J.; Majima, T.; Alvarez, P. J.; Choi, W.; Lee, J. Selective oxidative degradation of organic pollutants by singlet oxygen-mediated photosensitization: tin porphyrin versus C60 aminofullerene systems. *Environ. Sci. Technol.* **2012**, *46* (17), 9606−9613.
(15) Wöhrle, D.; Suvorova, O.; Gerdes, R.; Bartels, O.; Lapok, L.; Baziakina, N.; Makarov, S.; Slodek, A. Efficient oxidations and photooxidations with molecular oxygen using metal phthalocyanines as catalysts and photocatalysts. *J. Porphyrins Phthalocyanines* **2004**, *8* (8), 1020−1041.
(16) Mele, G.; Del Sole, R.; Vasapollo, G.; García-López, E.; Palmisano, L.; Schiavello, M. Photocatalytic degradation of 4-nitrophenol in aqueous suspension by using polycrystalline TiO_2 impregnated with functionalized Cu(II)−porphyrin or Cu(II)−phthalocyanine. *J. Catal.* **2003**, *217* (2), 334−342.
(17) Zhang, S.; Liu, X.; Wang, M.; Wu, B.; Pan, B.; Yang, H.; Yu, H. Q. Diketone-mediated photochemical processes for target-selective degradation of dye pollutants. *Environ. Sci. Technol. Lett.* **2014**, *1* (2), 167−171.
(18) Zakersalehi, A.; Nadagouda, M.; Choi, H. Suppressing NOM access to controlled porous TiO_2 particles enhances the decomposition of target water contaminants. *Catal. Commun.* **2013**, *41*, 79−82.
(19) Haag, W. R.; Yao, C. C. D. Rate constants for reaction of hydroxyl radicals with several drinking water contaminants. *Environ. Sci. Technol.* **1992**, *26* (5), 1005−1013.
(20) Turchi, C. S.; Ollis, D. F. Photocatalytic degradation of organic water contaminants: Mechanisms involving hydroxyl radical attack. *J. Catal.* **1990**, *122* (1), 178−192.
(21) Buxton, G. V.; Greenstock, C. L.; Helman, W. P.; Ross, A. B. Critical review of rate constants for reactions of hydrated electrons, hydrogen atoms and hydroxyl radicals (·OH/·O-) in aqueous solution. *J. Phys. Chem. Ref. Data* **1988**, *17* (2), 513−886.
(22) Zhao, D.; Chen, C.; Wang, Y.; Ji, H.; Ma, W.; Zang, L.; Zhao, J. Surface modification of TiO_2 by phosphate: Effect on photocatalytic activity and mechanism implication. *J. Phys. Chem. C* **2008**, *112* (15), 5993−6001.
(23) Frontistis, Z.; Drosou, C.; Tyrovola, K.; Mantzavinos, D.; Fatta-Kassinos, D.; Venieri, D.; Xekoukoulotakis, N. P. Experimental and modeling studies of the degradation of estrogen hormones in aqueous TiO_2 suspensions under simulated solar radiation. *Ind. Eng. Chem. Res.* **2012**, *51* (51), 16552−16563.
(24) Yang, K.; Lin, D.; Xing, B. Interactions of humic acid with nanosized inorganic oxides. *Langmuir* **2009**, *25* (6), 3571−3576.
(25) Sheng, H.; Li, Q.; Ma, W.; Ji, H.; Chen, C.; Zhao, J. Photocatalytic degradation of organic pollutants on surface anionized TiO_2: Common effect of anions for high hole-availability by water. *Appl. Catal., B* **2013**, *138−139*, 212−218.
(26) Valencia, S.; Marin, J. M.; Restrepo, G.; Frimmel, F. H. Application of excitation-emission fluorescence matrices and UV/Vis absorption to monitoring the photocatalytic degradation of commercial humic acid. *Sci. Total Environ.* **2013**, *442*, 207−14.
(27) O'Loughlin, E.; Chin, Y. P. Effect of detector wavelength on the determination of the molecular weight of humic substances by high-pressure size exclusion chromatography. *Water Res.* **2001**, *35* (1), 333−338.
(28) Wiszniowski, J.; Robert, D.; Surmacz-Gorska, J.; Miksch, K.; Weber, J. V. Photocatalytic decomposition of humic acids on TiO_2 Part I: Discussion of adsorption and mechanism. *J. Photochem. Photobiol., A* **2002**, *152* (1−3), 267−273.
(29) Al-Ajlouni, A. M. Indigo dyes as indicators for oxidation reactions: Competition kinetic studies. *Int. J. Chem. Kinet.* **2005**, *37*, 532−537.
(30) Sheng, H.; Ji, H.; Ma, W.; Chen, C.; Zhao, J. Direct four-electron reduction of O_2 to H_2O on TiO_2 surfaces by pendant proton relay. *Angew. Chem., Int. Ed.* **2013**, *52* (37), 9686−90.
(31) Pettibone, J. M.; Cwiertny, D. M.; Scherer, M.; Grassian, V. H. Adsorption of organic acids on TiO_2 nanoparticles: effects of pH, nanoparticle size, and nanoparticle aggregation. *Langmuir* **2008**, *24* (13), 6659−6667.
(32) Connor, P. A.; McQuillan, A. J. Phosphate adsorption onto TiO_2 from aqueous solutions: An in situ internal reflection infrared spectroscopic study. *Langmuir* **1999**, *15* (8), 2916−2921.
(33) Uyguner, C. S.; Bekbolet, M. Evaluation of humic acid photocatalytic degradation by UV−vis and fluorescence spectroscopy. *Catal. Today* **2005**, *101* (3−4), 267−274.
(34) Uyguner, C. S.; Bekbolet, M. Photocatalytic degradation of natural organic matter: Kinetic considerations and light intensity dependence. *Inter. J. Photoenergy* **2004**, *6* (2), 73−80.
(35) Han, Y.; Cheng, Q.; Chen, J.; Zhou, C.; Zhang, H.; Zhang, S.; Zhao, H. Extending the photoelectrocatalytic detection range of KHP by eliminating self-inhibition at TiO_2 nanoparticle electrodes. *J. Electroanal. Chem.* **2015**, *738*, 209−216.
(36) Li, X.; Li, J.; Bai, J.; Dong, Y.; Li, L.; Zhou, B. The inhibition effect of tert-butyl alcohol on the TiO_2 nano assays photoelectrocatalytic degradation of different organics and its mechanism. *Nano-Micro Lett.* **2016**, *8* (3), 221−231.
(37) Chen, X.; Zhang, Z.; Chi, L.; Nair, A. K.; Shangguan, W.; Jiang, Z. Recent advances in visible-light-driven photoelectrochemical water splitting: Catalyst nanostructures and reaction systems. *Nano-Micro Lett.* **2016**, *8* (1), 1−12.
(38) Abrantes, L. M.; Peter, L. M. Transient photocurrents at passive iron electrodes. *J. Electroanal. Chem. Interfacial Electrochem.* **1983**, *150* (1−2), 593−601.
(39) Zhao, H.; Jiang, D.; Zhang, S.; Wen, W. Photoelectrocatalytic oxidation of organic compounds at nanoporous TiO_2 electrodes in a thin-layer photoelectrochemical cell. *J. Catal.* **2007**, *250* (1), 102−109.
(40) Jiang, D.; Zhao, H.; Zhang, S.; John, R.; Will, G. D. Photoelectrochemical measurement of phthalic acid adsorption on porous TiO2 film electrodes. *J. Photochem. Photobiol., A* **2003**, *156* (1−3), 201−206.
(41) Brezonik, P. L.; Fulkerson-Brekken, J. Nitrate-induced photolysis in natural waters: Controls on concentrations of hydroxyl radical photo-intermediates by natural scavenging agents. *Environ. Sci. Technol.* **1998**, *32* (19), 3004−3010.
(42) Fujishima, A.; Zhang, X.; Tryk, D. A. TiO_2 photocatalysis and related surface phenomena. *Surf. Sci. Rep.* **2008**, *63* (12), 515−582.

DOI: 10.1021/acs.est.6b04845
Environ. Sci. Technol. 2017, 51, 514−521

(43) Ohtani, B. Photocatalysis A to Z—What we know and what we do not know in a scientific sense. *J. Photochem. Photobiol., C* **2010**, *11* (4), 157−178.
(44) Kang, S.; Xing, B. Humic Acid Fractionation upon Sequential Adsorption onto Goethite. *Langmuir* **2008**, *24* (6), 2525−2531.
(45) Baes, A. U.; Bloom, P. R. Diffuse Reflectance and Transmission Fourier Transform Infrared (DRIFT) Spectroscopy of Humic and Fulvic Acids. *Soil Sci. Soc. Am. J.* **1989**, *53* (3), 695−700.
(46) Plaschke, M.; Romer, J.; Klenze, R.; Kim, J. I. In situ AFM study of sorbed humic acid colloids at different pH. *Colloids Surf., A* **1999**, *160* (3), 269−279.
(47) Minero, C.; Mariella, G.; Maurino, V.; Pelizzetti, E. Photocatalytic transformation of organic compounds in the presence of inorganic anions. 1. Hydroxyl-mediated and direct electron-transfer Reactions of phenol on a titanium dioxide−fluoride System. *Langmuir* **2000**, *16* (6), 2632−2641.
(48) Sun, Y.; Pignatello, J. J. Evidence for a surface dual hole-radical mechanism in the titanium dioxide photocatalytic oxidation of 2,4-D. *Environ. Sci. Technol.* **1995**, *29* (8), 2065−2072.
(49) Moser, J.; Punchihewa, S.; Infelta, P. P.; Graetzel, M. Surface complexation of colloidal semiconductors strongly enhances interfacial electron-transfer rates. *Langmuir* **1991**, *7* (12), 3012−3018.

DOI: 10.1021/acs.est.6b04845
Environ. Sci. Technol. 2017, 51, 514−521